A 20-Year Dataset of Downwelling Longwave Flux at the Arctic Surface from TOVS Satellite Data

J. Francis
Rutgers University
New Brunswick, New Jersey

A. Schweiger
Polar Science Center
University of Washington
Seattle, Washington

J. Key
National Oceanic and Atmospheric Administration
National Environmental Satellite, Data, and Information Service
Madison, Wisconsin

Introduction

This paper summarizes the progress of a study under way to generate a 20-year dataset of surface downwelling longwave flux (DLF) retrievals from satellite data over the Arctic Ocean. We will produce daily fields between late 1979 and late 1998 on a grid with a spatial resolution of 100 km x 100 km^2 north of 60°N. Surface measurements from the Surface Heat Budget of the Arctic (SHEBA) and the Atmospheric Radiation Measurement (ARM) Program's North Slope of Alaska (NSA) site at Barrow, Alaska, are being used to validate the satellite-derived fluxes and to develop algorithm improvements in conditions that result in systematic errors.

During five months of the year when there is little or no solar radiation in the central Arctic basin, the surface energy budget is dominated by the net longwave flux. Recent model sensitivity studies, e.g., (Fischer and Lemke 1994; Ebert and Curry 1993; Thorndike 1992; and Makshtas and Timachev 1990), show that annual-average ice thickness is more sensitive to perturbations in longwave fluxes than in shortwave fluxes. Measurements of longwave fluxes over sea ice, however, are sparse and limited to points in space or to short periods in time. Existing satellite-derived estimates have large uncertainties owing to the failure of cloud detection algorithms to distinguish between clear and cloud-covered skies in conditions with near-surface temperature inversions and surface-based ice clouds, both of which occur frequently in the Arctic. Monthly mean fields have been derived from available data (e.g., Vowinkel and Orvig 1966, 1967; Khrol 1992), but to date little is known of the spatial variability on meso- or synoptic scales. (Schweiger and Key 1994) computed surface radiation fluxes in the Arctic from International Satellite Cloud Climatology Project (ISCCP) cloud data, but the accuracy of these fluxes in polar regions is questionable owing to significant disagreements between ISCCP cloud retrievals and surface-based climatologies.

If we are to improve our understanding of air-sea-ice interaction processes and sea ice evolution, with the ultimate goal of providing more realistic parameterizations for global climate models, estimates of the surface energy balance are required on shorter time and space scales and with more comprehensive areal coverage. In polar environments the most important factors determining surface downwelling longwave fluxes are cloud fraction, cloud thickness liquid water path (LWP) ice water path (IWP) (or LWP/IWP), and cloud-base temperature. The key to obtaining improved fields of this flux, therefore, is to acquire more accurate information about the clouds.

Method

We have developed a new technique to estimate the DLF from a combination of satellite sounder retrievals and brightness temperatures from the television and infrared observation satellite (TIROS) operational vertical sounder (TOVS), which has flown on National Oceanic and Atmospheric Administration (NOAA) polar-orbiting satellites continuously since late 1979. The fundamental concepts behind the methodology being used in this project have already been published (Francis 1997). We are performing further validation of the method using data from the Barrow, Alaska, ARM site, and the SHEBA field experiment, which was conducted in the Beaufort Sea from October 1997 to October 1998.

The DLF is computed from atmospheric temperature and moisture profiles, cloud fractions, and surface temperatures from TOVS. With funding from the NOAA/National Aeronautics and Space Administration (NASA) Pathfinder Project, we generated a 20-year TOVS Polar Pathfinder Dataset (Path-P) for the Arctic north of 60°N. The radiances were processed with a version of the Improved Initialization Inversion ("3I") algorithm (Chédin et al. 1985), (Scott et al. 1999) that has been modified to enhance accuracy over snow- and ice-covered surfaces (Francis 1994).

The TOVS retrievals have been extensively validated with data from field experiments (SHEBA, Coordinated Eastern Arctic Experiment [CEAREX], Arctic Leads ARI field Experiment [LeadEx]) and Russian NP station data (Schweiger et al. 2002). Accurate retrievals of cloud fraction and cloud base height are required for realistic estimates of DLF. This is not an easy task, however, owing to inherent differences between satellite and surface-based cloud observations (top-down versus bottom up view), point versus area-average values, and effects of varying cloud emissivity. As well as one can discern, the TOVS cloud retrievals appear to represent best estimates of cloud amount as reported by Ebert and Curry (1993) (pink line with asterisks in Figure 1). Figure 2 shows a comparison of TOVS (gridded Path-P) cloud fractions to a variety of other sources of cloud information.

In addition to temperature profiles, mean-layer moisture amounts, and cloud amount, we also use combinations of brightness temperatures from the high-resolution infrared radiation sounder (HIRS), which is one of the three sensors that composes TOVS. We use these to identify cloud phase, estimate cloud base height, and identify clouds below the near-surface temperature inversion. The primary innovation in the DLF approach is the use of sounding channels with differing sensitivity to cloud particles and heights of their weighting function peaks to estimate cloud thickness. In clear-sky conditions, two channels with peaks approximately 100 mb apart will exhibit the largest brightness temperature difference owing to the lapse rate of the atmosphere. If cloud particles are present, the difference between the channels decreases. The brightness temperature of the lower-peaking channel
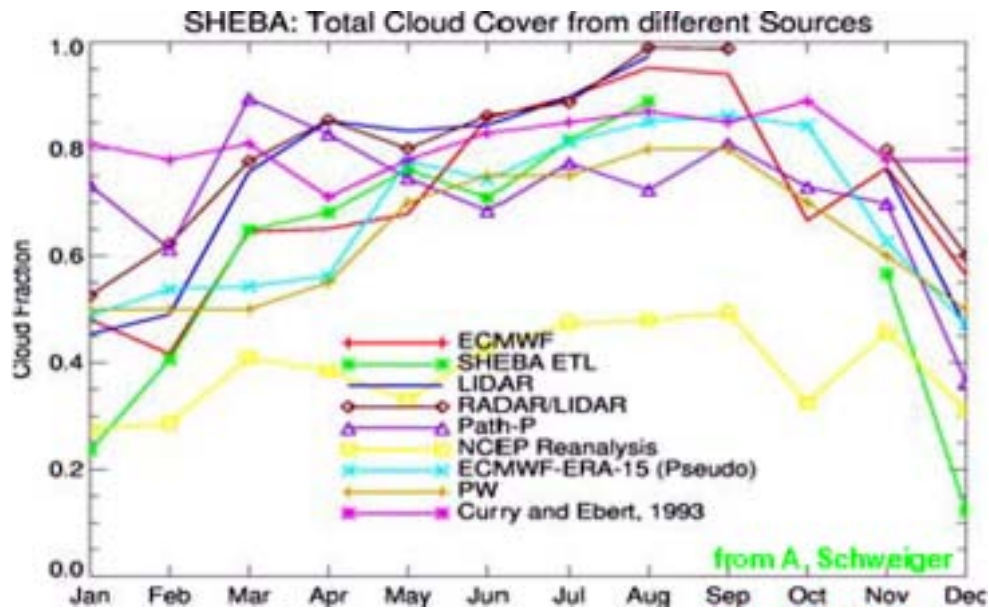
Figure 1. Comparison of cloud fraction climatologies over the annual cycle from a variety of surface-based, reanalysis, and satellite-retrieved datasets. The TOVS product is indicated as Path-P (purple line marked with triangles).

will decrease more than the upper one because more of its sensitivity function is affected by the cloud. As cloud particles increase, the difference between the channels also decreases. This range of differences is empirically related to a geometric cloud thickness extending below the TOVS-retrieved cloud top. Two pairs of channels, one for lower, and one for higher clouds are used for cloud thickness estimates. Of course, once the cloud becomes optically thick, the channel difference becomes constant and a maximum thickness is assumed. This is undoubtedly a crude estimate of cloud thickness, but existing algorithms routinely assume that cloud thickness is constant – typically 50 hPa. The 50-hPa assumption has been shown to be unsuitable for Arctic conditions and large errors in DLF result.

The original DLF method ingested the satellite information into a forward radiative transfer model called Streamer (Key and Schweiger 1998). Soon after embarking on this project, however, it became clear that to process 20 years of level-2 (orbital swath) satellite retrievals, a tremendous amount of computer resources would be required. Consequently, we have adapted the DLF algorithm to a neural network version of a forward radiative transfer model called FluxNet (Key and Schweiger 1998). The neural network method increases the computing speed by a factor of 10 with no perceptible decrease in accuracy.

Preliminary Results

Figure 2 shows a comparison of TOVS-derived longwave fluxes to those measured at the SHEBA camp from January through October 1998. Correlation between the two time series is 0.86 with a bias of 3.2 Wm^{-2}. We recognize that perfect agreement is impossible, as satellite retrievals integrate conditions
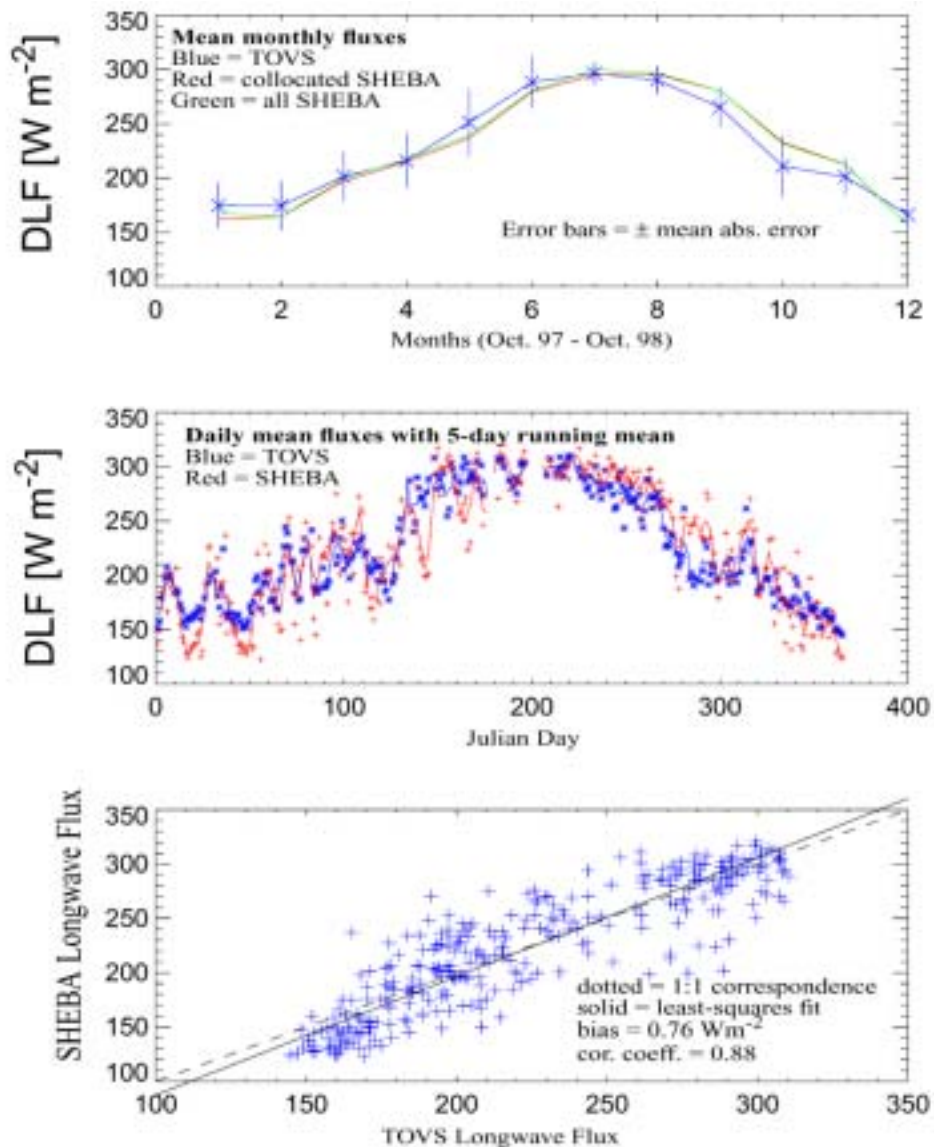
Figure 2. Comparison of TOVS-derived downwelling longwave flux to DLF measured at SHEBA. Top panel shows monthly means over annual cycle, middle is time series of individual comparisons with superimposed 5-day running mean, and bottom is scatterplot of collocated daily values.

over a $(100\text{-km})^2$ area, while SHEBA measurements are made at a point in time and space. This incompatibility should result in the extremes being damped by the satellite retrievals, which is exactly what we see in these comparisons. Comparisons of daily covariability in DLF and surface temperatures from SHEBA measurements and TOVS-derived quantities suggest that the relationship between these two variables is not as intimate as it should be. This is likely due to the large area represented by each TOVS retrieval (100×100 km^2), which would include a variety of ice thicknesses, leads, and cloud types around the SHEBA site. The SHEBA values, in contrast, are at a single point over thick pack ice.

Our preliminary comparisons to measurements at the ARM site in Barrow, Alaska, appear somewhat less encouraging, but the differences may occur for good reasons. Figure 3 illustrates a comparison of daily-mean surface-measured DLF with TOVS-derived values for all of 1999. All TOVS retrievals within a 24-hour period centered on 12 Universal Time Coordinates (UTC) and within 100 km of the ARM site are averaged and compared with ARM measurements that are also averaged over 24 hours. Gaps in the TOVS retrievals occur on days with heavy overcast, which occurs more frequently in summer.
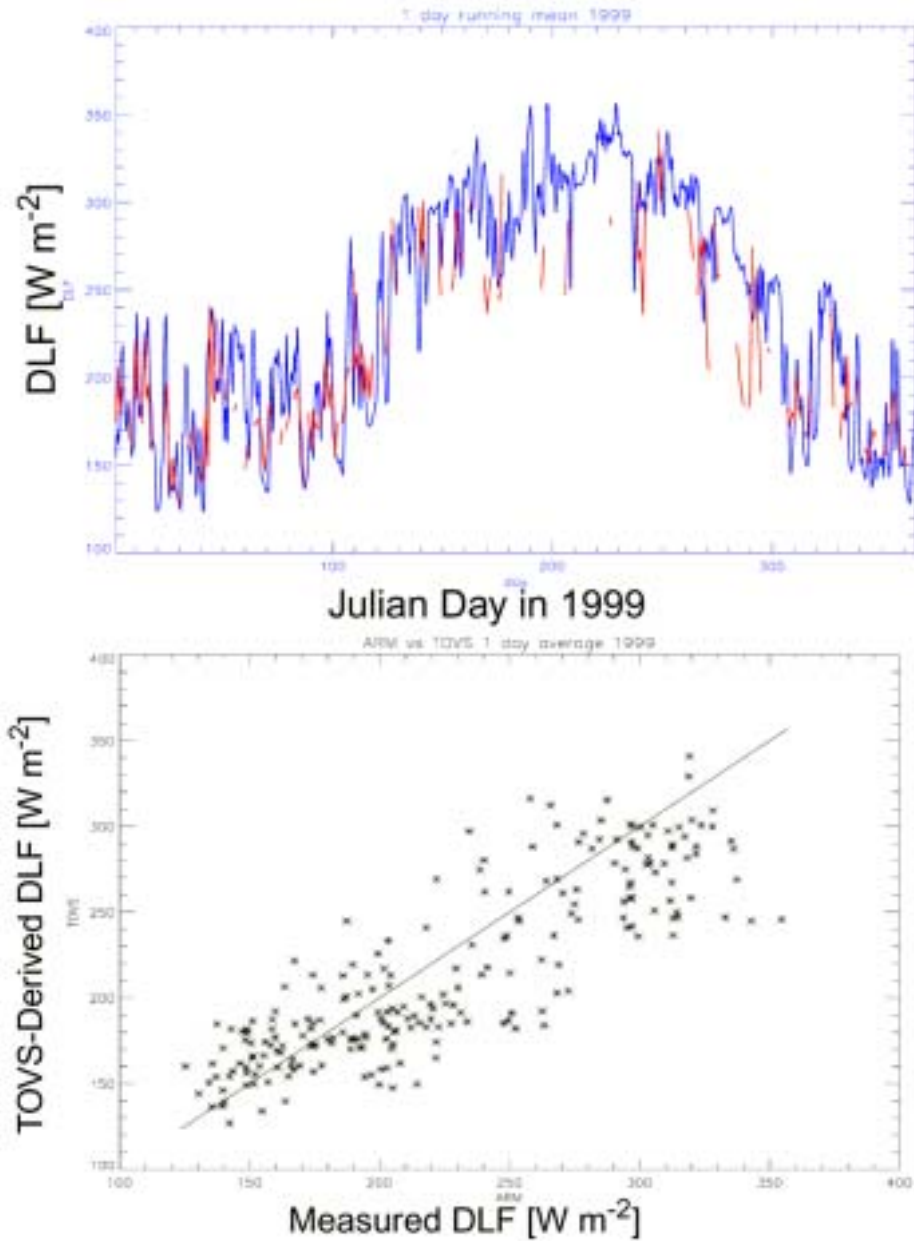

Figure 3. Comparison of daily mean DLF values measured at the ARM site in Barrow, Alaska and retrieved from TOVS satellite data within 100 km of the ARM site. The upper plot is a time series over all days in 1999, and the lower panel is a scatter plot.

As with the SHEBA comparison, we see that the TOVS-derived values exhibit a smaller range than the measurements. Unlike at SHEBA, the TOVS DLFs are consistently too low in summer, contributing to a negative bias of about -11 Wm^{-2}. This is also not unexpected, as the 100-km radius of accepted TOVS retrievals that enter into the averaging calculation include values over the ocean and sea ice, which will generally have lower DLFs than snow-free, land at Barrow where the measurements are made. Surface air temperatures in Barrow are about 5° to 10°C in summer, while over the ocean and sea ice they would hover near the freezing point of water. Higher air temperatures over land would lead to larger DLF measurements. Finally, we present an example of our anticipated product: Arctic-wide fields of DLF. Here we show the monthly averaged DLF for March 1999 (Figure 4).
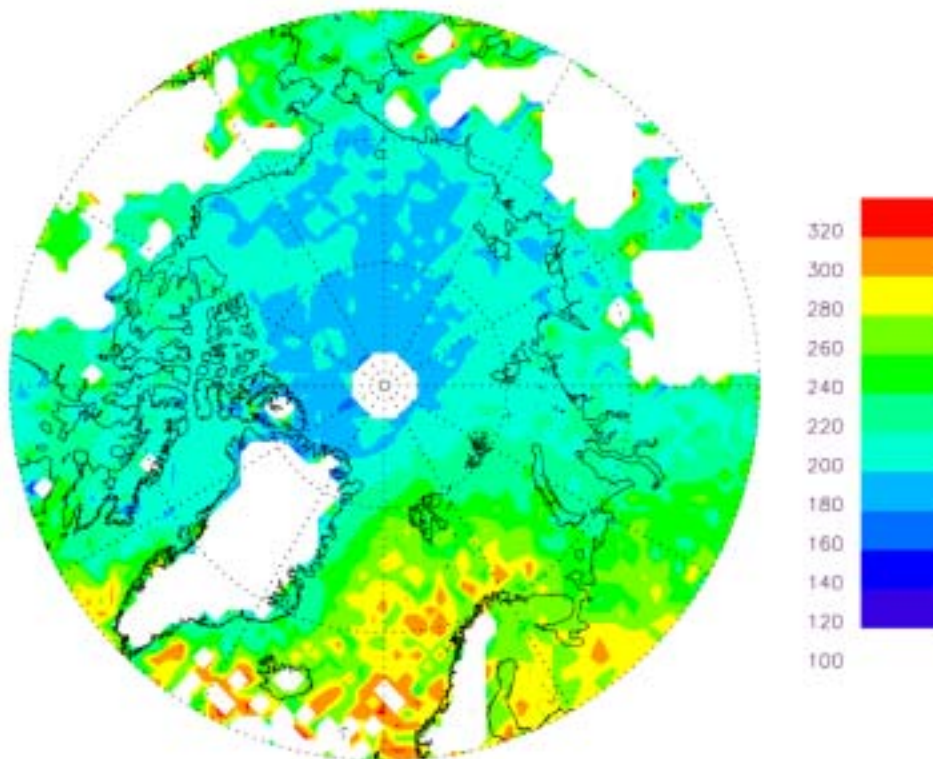

Figure 4. Mean DLF for March 1999 derived from TOVS retrievals and brightness temperatures.

Future Work

Validation efforts will continue in hopes of reducing errors in retrieved fluxes during conditions when discrepancies with surface observations are large. We will use surface-based lidar and radar retrievals from SHEBA and the ARM site to identify cloud conditions in ambiguous cases. The full 20 years of TOVS data will be processed to produce daily, Arctic-wide fields of DLF for driving sea ice models, validating climate model products, and analyzing apparent changes in related climate variables. We hope to archive the data at NSIDC for easy access by the entire scientific community.

Acknowledgments

Corresponding Author

Jennifer Francis, francis@imcs.rutgers.edu, (732) 708-1217

References

Chédin, A., N. A. Scott, C. Wahiche, and P. Moulineir, 1985: The Improved Initialization Inversion method: A high resolution physical method for temperature retrievals from satellites of the TIROS-N series. *J. Clim. Appl. Meteorol.,* **24**, 128-143.

Ebert, E. E., and J. A. Curry, 1993: An intermediate one-dimensional thermodynamic sea ice model for investigating ice-atmosphere interactions. *J. Geophys. Res.*, **98**, 10,085-10,109.

Fischer, H., and P. Lemke, 1994: On the required accuracy of atmospheric forcing fields for driving dynamic-thermodynamic sea ice models, in *The Polar Oceans and Their Role in Shaping the Global Environment, Geophys. Monogr.* Ser., vol. 85, eds. O. M. Johannessen, R. D. Muench, and J. E. Overland, pp. 373-381, AGU, Washington, D.C.

Francis, J. A., 1997: A method to derive longwave fluxes at the Arctic surface from TIROS operational vertical sounder data. *J. Geophys. Res.*, **102**, 1795-1806.

Francis, J. A., 1994: Improvements to TOVS retrievals over sea ice and applications to estimating Arctic energy fluxes. *J. Geophys. Res.*, **99**, 10,395-10,408.

Key, J., and A. J. Schweiger, 1998: Tools for atmospheric radiative transfer: Streamer and FluxNet. *Computers and Geosciences*, **24**(5), 443-451.

Khrol, V. P. (Ed.), 1992: *Atlas of the Energy Balance of the Northern Polar Area,* Arctic, and Antarctic. Res. Inst., p. 72, St. Petersburg, Russia.

Makshtas, A. P., and V. F. Timachev, 1990: Sensitivity of a thermodynamic model of sea ice to parameterization of short- and long-wave radiation, in *Report on a Workshop on Polar Radiation Fluxes and Sea-Ice Modeling*, eds. E. Raschke, H. Cattle, P. Lemke, and W. Rossow, p. 67, World Clim. Res. Programme. *Sea Ice and Clim.*, Bremerhaven, Germany.

Schweiger, A. J., and J. R. Key, 1994: Arctic Ocean radiative fluxes and cloud forcing estimated from the ISCCP-C2 cloud dataset, 1983-1990. *J. Appl. Meteor.*, **33**, 948-963.

Schweiger, A. J., R. W. Lindsay, J. A. Francis, J. Key, J. Intrieri, and M. Shupe, 2002: Validation of TOVS Path-P data during SHEBA. *J. Geophys. Res.*, **107**(C10), 8041, 10.1029/2000JC000453.

Scott, N. A., A. Chedin, R. Armante, J. Francis, C. Stubenrauch, J.-P. Chaboureau, F. Chevallier, C. Claud, and F. Cheruy, 1999: Characteristics of the TOVS Pathfinder Path-B dataset. *Bull. Am. Meteor. Soc.*, **80**, 2679-2701.

Thorndike, A. J., 1992: A toy model linking atmospheric thermal radiation and sea ice growth. *J. Geophys. Res.,* **97**, 9401-9410.

Vowinckel, E., and S. Orvig, 1966: *Energy balance of the Arctic, 5*, The heat budget of the Arctic Ocean. *Arch. Meteorol. Geophys. Bioklimatol.,* Ser. A, **14**, 303-325.

Vowinckel, E., and S. Orvig, 1967: Climate change over the Polar Ocean, 1, The radiation budget. *Arch. Meteorol. Geophys. Bioklimatol.,* Ser. A, **15**, 1-23, 1967.